OUTP-12-15P

The impact of heavy-quark loops on LHC dark matter searches

Ulrich Haisch,[1,*] Felix Kahlhoefer,[1,†] and James Unwin[1,2,‡]
[1] *Rudolf Peierls Centre for Theoretical Physics, University of Oxford,*
1 Keble Road, Oxford OX1 3NP, United Kingdom
[2] *Mathematical Institute, University of Oxford, 24-29 St Giles, Oxford, OX1 3LB, UK*

(Dated: August 24, 2012)

If only tree-level processes are included in the analysis, LHC monojet searches give weak constraints on the dark matter-proton scattering cross section arising from the exchange of a new heavy scalar or pseudoscalar mediator with Yukawa-like couplings to quarks. In this letter we calculate the constraints on these interactions from the CMS $5.0\,\mathrm{fb}^{-1}$ and ATLAS $4.7\,\mathrm{fb}^{-1}$ searches for jets with missing energy including the effects of heavy-quark loops. We find that the inclusion of such contributions leads to a dramatic increase in the predicted cross section and therefore a significant improvement of the bounds from LHC searches.

arXiv:1208.4605v1 [hep-ph] 22 Aug 2012

I. INTRODUCTION

It is a remarkable fact that one of the leading experiments for dark matter (DM) detection is the LHC. Although any DM particles produced at the LHC will escape from the detector unnoticed, we may observe large amounts of missing transverse energy ($\not\!\!E_T$) if a single jet (j) is produced in association with a pair of DM particles. The experimental search for such monojet events provides model-independent bounds on the interaction strength of DM with quarks and gluons, constraining the same parameters as direct detection experiments [1, 2]. These searches place the leading (and in some cases only) limits on models of DM over certain regions of parameter space.

If the mediator of the DM interaction is sufficiently heavy, it can be integrated out to obtain an effective higher-dimensional operator that describes the low-energy interactions between DM and Standard Model (SM) states. For instance, the interactions of a fermionic DM particle ψ with SM quarks q via a heavy scalar mediator Φ with quark couplings proportional to the quark mass m_q can be described by the four-fermion operator

$$\mathcal{O}_s^\psi = \frac{m_q}{\Lambda_s^3}\,\bar{q}q\,\bar{\psi}\psi\;, \tag{1}$$

and the DM pair production proceeds through tree-level diagrams like those shown on the left in Fig. 1. Unfortunately, the suppression scale Λ_s in (1) is very difficult to constrain with LHC monojet searches [3–10] since the initial state contains (apart from gluons) only light quarks, which by assumption have small couplings to the scalar mediator Φ.

In this letter we observe that the situation changes dramatically beyond tree level, since now loop graphs involving virtual top quarks give rise to a $j + \not\!\!E_T$ signal. Examples of such Feynman diagrams are displayed on the right in Fig. 1. We find that by including these loop contributions, the predicted cross section for monojet production increases by more than two orders of magnitude leading to bounds on Λ_s which are about a factor of 3 stronger than the constraints from the simple tree-level analysis with DM-quark operators. To our knowledge, this important observation has not been made before.

This paper is structured as follows: in Sec. II, we present the various operators which we intend to examine. In Sec. III we calculate the constraints arising from the latest LHC searches for jets with $\not\!\!E_T$, including the full top-quark mass dependence of the squared matrix elements for DM pair + jet production. Our calculation is performed at the leading order (LO) in QCD, but we will comment on the importance of higher-order effects as well as the applicability of the heavy top-quark approximation. Finally, in Sec. IV we discuss the impact of the enhanced monojet limits in the context of relic density constraints and recent results from direct detection experiments.

II. EFFECTIVE OPERATORS

Our focus will be on interactions that result from the exchange of a new heavy scalar or pseudoscalar state which connects SM quarks to DM. In the case that the scalar mediator is a SM singlet it can couple to quarks via mixing with the Higgs and the induced couplings will be proportional to the SM Yukawa couplings:

$$\mathcal{L}_\Phi = g_q\,\frac{m_q}{v}\,\bar{q}q\,\Phi + g_\psi\,\bar{\psi}\psi\,\Phi\;, \tag{2}$$

where $v \simeq 246\,\mathrm{GeV}$ is the Higgs vacuum expectation value. Integrating out the mediator Φ, we obtain the effective interaction (1) and the scale Λ_s is related to the fundamental couplings by $\Lambda_s^3 = v M_\Phi^2/(g_q g_\psi)$. If DM is a scalar ϕ rather than a fermion ψ, we obtain in complete analogy the effective operator

$$\mathcal{O}_s^\phi = \frac{m_q}{\Lambda_s^2}\,\bar{q}q\,\phi^\dagger\phi\;. \tag{3}$$

---

[*] u.haisch1@physics.ox.ac.uk

[†] felix.kahlhoefer@physics.ox.ac.uk

[‡] j.unwin1@physics.ox.ac.uk

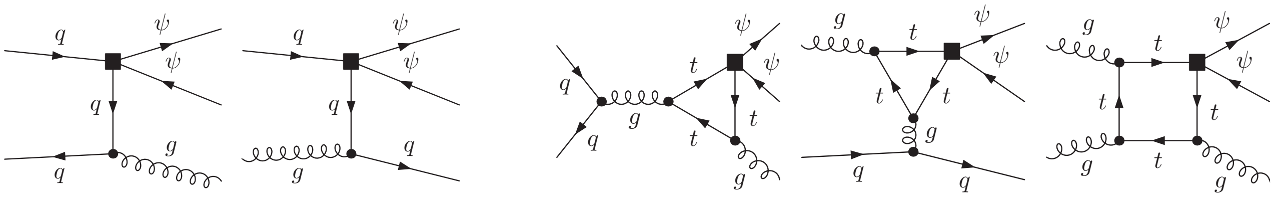

FIG. 1. Typical tree-level (left) and loop-level (right) diagrams leading to monojet events. The black squares denote insertions of four-fermion operators.

The other type of portal interaction for which the effective operator may naturally have Yukawa-like couplings involves heavy pseudoscalar mediators. The corresponding effective operator is [11]

$$\mathcal{O}_p^\psi = \frac{m_q}{\Lambda_p^3}\, \bar{q}\gamma^5 q\, \bar{\psi}\gamma^5\psi \; . \tag{4}$$

This case is of particular interest, since direct detection signals associated to $\mathcal{O}_p^\psi$ are spin-dependent and suppressed by powers of $q/m_N \ll 1$, where q is the momentum transfer and m_N is the mass of the target nucleus. Thus, monojet searches provide the only manner to obtain constraints on Λ_p for the foreseeable future.

III. LIMITS FROM MONOJET SEARCHES

In their most recent analysis with an integrated luminosity of $5.0\,\text{fb}^{-1}$ at $\sqrt{s} = 7\,\text{TeV}$ the CMS collaboration [1] found no apparent excesses in their searches for jets with $\not{E}_T$ providing the leading monojet bounds on DM. CMS considered events with $\not{E}_T > 350\,\text{GeV}$, provided there was a primary jet (j_1) with transverse momentum $p_T > 110\,\text{GeV}$ and pseudorapidity $|\eta| < 2.4$. A secondary jet (j_2) with $p_T > 30\,\text{GeV}$ was also permitted if the two jets are not back-to-back: $|\Delta\phi(j_1, j_2)| < 2.5$. Events with high-$p_T$ tertiary jets, electrons or muons were vetoed. This null result excludes new contributions to the production cross section in excess of 0.032 pb at 95% confidence level (CL). The ATLAS search [2] employs very similar cuts and finds a comparable bound on the cross section. We have checked explicitly that using the ATLAS data instead of the CMS data does not modify our results within errors.

To calculate the predicted monojet cross section for the operators introduced above we have implemented each of them in `FeynArts` [12] and performed the computations with `FormCalc` and `LoopTools` [13]. Furthermore, as an independent cross-check, we have verified our findings with `MCFM` [14], modifying the process $p + p \to H\,(A) + j \to \tau^+\tau^- + j$, which is based on the analytical results of [15] for the scalar Higgs case and [16] for the pseudoscalar Higgs case. Both computations utilise `MSTW2008LO` parton distributions [17]. In our calculations we do not consider the effects of parton showering and hadronisation or the contribution of additional jets. As discussed in [4, 18], the first two simplifications are justified, because the primary jet has sufficiently high p_T, which renders the impact of non-hard QCD radiation small. We will comment on the effect of two-jet events below.

m_{DM} [GeV]	Λ_s^ψ [GeV]	Λ_p^ψ [GeV]	Λ_s^ϕ [GeV]
10	148^{+12}_{-11}	164^{+14}_{-11}	63^{+8}_{-6}
100	145^{+12}_{-10}	164^{+14}_{-12}	61^{+8}_{-6}
200	136^{+12}_{-10}	160^{+13}_{-12}	56^{+7}_{-6}
500	97^{+9}_{-7}	122^{+10}_{-9}	30^{+4}_{-3}
1000	50^{+5}_{-4}	68^{+7}_{-5}	10^{+1}_{-1}

TABLE I. Bounds on Λ at 95% CL from the CMS $5.0\,\text{fb}^{-1}$ search for jets with $\not{E}_T$ including loop-level processes in the analysis. The quoted errors reflect the scale uncertainties. See text for details.

Our results are summarised in Tab. I and displayed in Fig. 2 for the case where DM is either a Dirac fermion or a complex scalar. For Majorana fermion or real scalar DM, the predicted cross sections are larger by a factor of 2 and so the bounds on Λ are stronger by roughly 12%. For the scalar (pseudoscalar) operators we find that including the loop-level processes in the calculation increases the predicted monojet cross sections by a factor of around 500 (900), the precise value depending on the DM mass and the choices of renormalisation (μ_R) and factorisation (μ_F) scales. These numbers translate into an increase of the bounds on Λ by a factor of 2.8 (3.1). Note that the limit on Λ_s which we obtain from the tree-level processes alone is stronger than the one reported in [2] by about 25%, because we include bottom quarks in the initial state, which we find to give the dominant contribution at tree level.

Before examining the impact of additional QCD radiation, we first discuss whether the above results could have been obtained without performing an actual loop calculation, but rather by employing the heavy top-quark mass limit. For the operator $\mathcal{O}_s^\psi$, the effect of heavy-quark loops can be described in this approximation in terms of the effective operator

$$\mathcal{O}_{sg}^\psi = \frac{\alpha_s}{4\Lambda_g^3}\, G^a_{\mu\nu} G^{a\,\mu\nu}\, \bar{\psi}\psi \; . \tag{5}$$

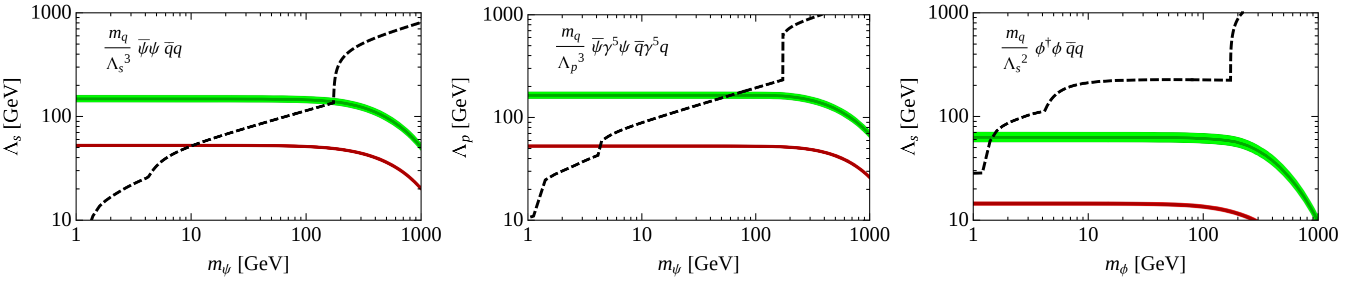

FIG. 2. LHC monojet bounds on the scale Λ at tree-level (red) and loop-level (green) for the effective operators $\mathcal{O}_s^\psi$, $\mathcal{O}_p^\psi$, and $\mathcal{O}_s^\phi$ (from left to right). The black dashed curves indicate the requirement for the correct relic density. The width of the bands reflect the scale uncertainties. See text for details.

The operator induced by $\mathcal{O}_s^\phi$ ($\mathcal{O}_p^\psi$) is obtained by replacing $\bar\psi\psi$ with $\phi^\dagger\phi$ ($G^a_{\mu\nu}G^{a\,\mu\nu}$ with $G^a_{\mu\nu}\tilde G^{a\,\mu\nu}$). Effective interactions like (5) have been studied previously in the context of monojet searches [3, 5, 8, 9]. In fact, for $m_t \to \infty$ bounds on these operators can be translated into limits on $\mathcal{O}_s^{\psi,\phi}$ and $\mathcal{O}_p^\psi$ by the simple identifications $\Lambda_s = \Lambda_g/(3\pi)^{1/3}$ and $\Lambda_p = \Lambda_g/(2\pi)^{1/3}$.

The scales involved in $j + \not\!\!E_T$ production (i.e. the p_T and the DM mass) are, however, not necessarily small compared to the top-quark mass, which implies that the infinite mass limit employed to obtain (5) is not a good approximation [19]. Numerically, we find that applying the $m_t \to \infty$ limit overestimates the monojet cross sections by a factor of around 3 for small DM mass and that the quality of the approximation rapidly degrades with increasing p_T cut and DM mass, resulting in errors of up to a factor of 40. These numbers imply that the corresponding limits on Λ would be too strong by a factor of 1.2 (1.9) in the best (worst) case. This clearly shows that one cannot use $\mathcal{O}_{sg}^\psi$ (or analogous operators) to infer faithful bounds on the quark-DM contact operators.

To assess the theoretical errors in our analysis, we have studied the scale ambiguities of our results. We find the scale μ which determines $\alpha_s(\mu)$ dynamically, i.e. we define $\mu = \xi\, p_T = \mu_R = \mu_F$ and evaluate it on an event-by-event basis. Following common practice, we have varied ξ in the range $[\frac{1}{2}, 2]$. We find that the predictions of the tree-level and loop-level monojet cross sections calculated in this way vary by around $\pm 20\%$ and $\pm 50\%$, respectively. The resulting uncertainties on Λ stay below $\pm 2\,\text{GeV}$ and $\pm 15\,\text{GeV}$. They are given in Tab. I and reflected by the width of the coloured bands in Fig. 2.

The pronounced scale ambiguity of the loop-level result indicates that next-to-leading order (NLO) corrections might be large. Indeed, the K-factor representing the ratio between the NLO and LO cross sections of $p + p \to H + j$ evaluated in the $m_t \to \infty$ limit, varies between 1.2 and 1.8 depending on the kinematic region and choice of parton densities [20–22]. Using `MCFM`, we explicitly verified that the same range of K-factors also apply to the monojet signal, although the imposed p_T cut is significantly higher in this case than in the case of Higgs + jet production.

Another important and related issue is the relevance of events with a second high-p_T jet. Such events are allowed in the CMS analysis, as long as the two jets are not back-to-back. To estimate the cross section for events with two jets and $\not\!\!E_T$, we use the cross section for $H + 2j$ implemented into MCFM in the limit $m_t \to \infty$ [23, 24]. This limit is known to work better in the case of $H + 2j$ than for $H + j$ [25]. We find that the dominant contribution to two-jet events arises from processes that resemble monojet events but have an additional gluon in the final state. Allowing a second jet with large p_T increases the total cross section by about a factor of 2, consistent with the more accurate simulations from CMS [1].

The inclusion of NLO corrections and of two-jet events is hence expected to strengthen the bounds on Λ, possibly by as much as 25%. However, we expect this improvement to be somewhat smaller in the full calculation with resolved top-quark loops (in particular, for high p_T cut and large DM mass), so we prefer not to include these effects in our results and give a conservative bound. Clearly, a more careful analysis of finite top-quark mass effects at $\mathcal{O}(\alpha_s^4)$ (along the lines of the recent Higgs + jet study [26]) is required to make a more quantitative statement. This study is left for future work.

Finally, we note that the values of Λ that we can exclude with the current data are relatively low compared to typical LHC energies and thus we anticipate that the new scalar or pseudoscalar mediator may be produced on-shell in pp collisions, unless the couplings g_q and g_ψ in (2) are large (see [8, 9, 27]). In this case the analysis becomes more model-dependent and monojet bounds may be modified [28]. With increasing integrated luminosity, however, the bounds on Λ will improve, making the method advocated here more reliable.

IV. DISCUSSION

The suppression scale Λ which can be constrained through monojet searches also enters in the formula for the DM annihilation cross section into quarks and the DM-proton scattering cross section. Consequently, limits on Λ can also be inferred from measurements of the relic density and DM direct detection experiments. Here we compare these results with the bounds derived in the previous section.

The annihilation cross sections for the three operators introduced in Sec. II are given e.g. in [10]. Using the expansion $\langle \sigma v \rangle = a + 6b/x + \mathcal{O}(1/x^2)$ with $x = m_{\rm DM}/T$, the DM relic density $\Omega_{\rm DM}$ after freeze-out is given by [29]

$$\Omega_{\rm DM} h^2 \simeq \frac{1.07 \times 10^9}{\rm GeV} \frac{x_f}{M_{\rm Pl} \sqrt{g_*} \left(a + \frac{3b}{x_f} \right)} \,, \qquad (6)$$

where g_* is the number of relativistic degrees of freedom at the freeze-out temperature T_f. The coefficients a and b are functions of Λ and $m_{\rm DM}$. If we assume that the interactions between the DM particle and SM quarks are the dominant ones at freeze-out, we can determine Λ as a function of $m_{\rm DM}$ by the requirement that the observed DM relic abundance $\Omega_{\rm DM} h^2 \simeq 0.1109$ [30] is reproduced.

The values of Λ which give the correct relic density are indicated by the black dashed curves in Fig. 2. From the intersections of the monojet bounds and the relic density constraints, we obtain the following lower bounds on the DM mass:

$$\begin{aligned} \mathcal{O}_s^\psi : &\quad m_\psi > 173 \; (174) \; {\rm GeV} \,, \\ \mathcal{O}_p^\psi : &\quad m_\psi > 60 \; (85) \; {\rm GeV} \,, \qquad (7) \\ \mathcal{O}_s^\phi : &\quad m_\phi > 1.5 \; (1.6) \; {\rm GeV} \,. \end{aligned}$$

Here the values in brackets apply if DM is a Majorana fermion or a real scalar instead of a Dirac fermion or a complex scalar. Note that the relic abundance requirements may differ in alternative frameworks, for instance asymmetric DM (see e.g. [10]). Also, additional annihilation channels, e.g. into leptons, gauge bosons or new hidden sector states, may avoid an overproduction of DM and therefore help reduce tension with experiments.

For the scalar operators $\mathcal{O}_s^\psi$ and $\mathcal{O}_s^\phi$, the DM direct detection cross section is given by

$$\sigma_p^\psi = \frac{\mu_p^2 \, m_p^2}{\pi} \frac{f^2}{\Lambda^6} \,, \qquad \sigma_p^\phi = \frac{\mu_p^2 \, m_p^2}{\pi} \frac{f^2}{\Lambda^4 \, m_\phi^2} \,, \qquad (8)$$

where m_p is the proton mass, μ_p is the DM-proton reduced mass and $f \simeq 0.35$ is the scalar form factor of the proton [31]. The scattering cross sections for Majorana or real scalar DM are larger by a factor of 4. Utilizing the formulas (8), the monojet bounds on Λ can be translated into limits on σ_p, which in turn can be compared to the exclusion limits obtained from XENON100 [32], XENON10 [33] and CDMS-II [34, 35] as well as to the best-fit regions obtained from DAMA [36] and CoGeNT [37] [38].

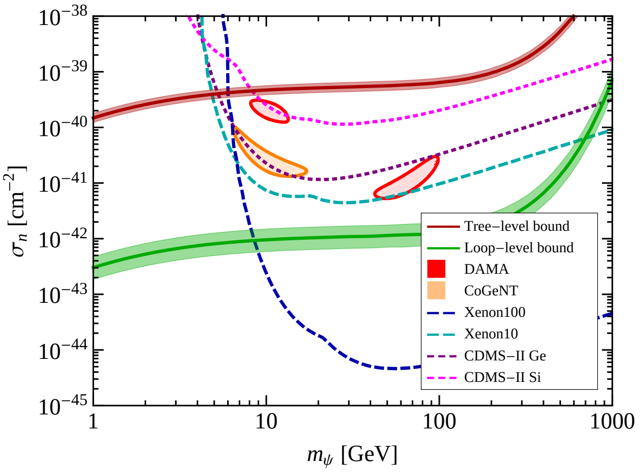

FIG. 3. LHC monojet bounds on the DM-proton cross section for the operator $\mathcal{O}_s^\psi$ at tree-level (red) and loop-level (green) compared to various results from DM direct detection experiments. While the tree-level monojet bound is too weak to constrain the parameter regions favoured by DAMA and CoGeNT, the loop-level bound clearly excludes these regions.

Our final results are shown in Fig. 3 for the case where the DM particle is a Dirac fermion. All shown bounds and best-fit regions represent 95% CL ranges. For large values of m_ψ, as indicated by the relic density constraints, direct detection experiments give stronger bounds than monojet searches. For $m_\psi \simeq 10\,{\rm GeV}$, the bounds become comparable, while below this value the bounds from LHC searches are far superior. We observe that the inclusion of loop-level processes gives a pertinent improvement of the monojet bounds, in particular because it excludes the possibility that the CoGeNT excess or the DAMA modulation arise from the interactions of a heavy scalar mediator.

For the pseudoscalar operators the DM direct detection cross section is spin-dependent and suppressed by q^4/m_p^4, so that no relevant bounds on Λ can be obtained from direct detection experiments. Consequently, the bounds shown in the central panel of Fig. 2 are presently the strongest limit on the new-physics scale Λ. It is evident from the figure that including one-loop contributions improves the bound on m_ψ inferred from the relic abundance by a factor of approximately 15.

In summary, while collider bounds on DM-quark contact operators with Yukawa-like couplings are relatively weak when only tree-level processes are considered, much stronger bounds can be obtained by including heavy-quark loops in the analysis. In this letter, we used the recent CMS $5.0\,{\rm fb}^{-1}$ and ATLAS $4.7\,{\rm fb}^{-1}$ searches for jets with $\not{E}_T$ to obtain the strongest collider limits on mass-dependent DM-quark scalar and pseudoscalar contact operators. Given that the LHC high-p_T experiments are rapidly accumulating luminosity, constraints on all contact operators involving DM particles with masses below the electroweak scale will improve significantly in the near future. The methods outlined here will be important for further advances in constraining the parameter space of DM-quark interactions with mass-dependent couplings, and we are looking forward to their implementation in future LHC analyses.

Acknowledgements: We are grateful to Keith Ellis, Mads Frandsen, Robert Harlander, John March-Russell, Michael Rauch, Raoul Rontsch, Subir Sarkar, Kai Schmidt-Hoberg, Alex Tapper, Stephen West, Steven Worm and Giulia Zanderighi for useful discussions. UH acknowledges travel support from the UNILHC network (PITN-GA-2009-237920). FK is supported by the Studienstiftung des Deutschen Volkes. JU is grateful for partial support from the Esson Bequest, Mathematical Institute, Oxford and the Vice-Chancellors' Fund, Oxford.

---

[1] S. Chatrchyan *et al.* (CMS Collaboration), (2012), arXiv:1206.5663.

[2] ATLAS Collaboration, ATLAS-CONF-2012-084.

[3] J. Goodman, M. Ibe, A. Rajaraman, W. Shepherd, T. M. Tait, *et al.*, Phys.Lett. **B695**, 185 (2011), arXiv:1005.1286.

[4] Y. Bai, P. J. Fox, and R. Harnik, JHEP **1012**, 048 (2010), arXiv:1005.3797.

[5] J. Goodman, M. Ibe, A. Rajaraman, W. Shepherd, T. M. Tait, *et al.*, Phys.Rev. **D82**, 116010 (2010), arXiv:1008.1783.

[6] P. J. Fox, R. Harnik, J. Kopp, and Y. Tsai, Phys.Rev. **D84**, 014028 (2011), arXiv:1103.0240.

[7] A. Rajaraman, W. Shepherd, T. M. Tait, and A. M. Wijangco, Phys.Rev. **D84**, 095013 (2011), arXiv:1108.1196.

[8] P. J. Fox, R. Harnik, J. Kopp, and Y. Tsai, Phys.Rev. **D85**, 056011 (2012), arXiv:1109.4398.

[9] P. J. Fox, R. Harnik, R. Primulando, and C.-T. Yu, Phys.Rev. **D86**, 015010 (2012), arXiv:1203.1662.

[10] J. March-Russell, J. Unwin, and S. M. West, JHEP **1208**, 029 (2012), arXiv:1203.4854.

[11] For brevity, we omit the case of scalar DM with a pseudoscalar mediator, since this interaction violates CP, making this scenario rather less appealing. Note, however, that the limits for this operator would be comparable to those presented.

[12] T. Hahn, Comput.Phys.Commun. **140**, 418 (2001), arXiv:hep-ph/0012260.

[13] T. Hahn and M. Perez-Victoria, Comput.Phys.Commun. **118**, 153 (1999), arXiv:hep-ph/9807565.

[14] J. Campbell, R. K. Ellis, and C. Williams, `http://mcfm.fnal.gov`.

[15] R. K. Ellis, I. Hinchliffe, M. Soldate, and J. van der Bij, Nucl.Phys. **B297**, 221 (1988).

[16] M. Spira, A. Djouadi, D. Graudenz, and P. Zerwas, Nucl.Phys. **B453**, 17 (1995), arXiv:hep-ph/9504378.

[17] A. Martin, W. Stirling, R. Thorne, and G. Watt, Eur.Phys.J. **C63**, 189 (2009), arXiv:0901.0002.

[18] G. Choudalakis, (2011), arXiv:1110.5295.

[19] U. Baur and E. N. Glover, Nucl.Phys. **B339**, 38 (1990).

[20] D. de Florian, M. Grazzini, and Z. Kunszt, Phys.Rev.Lett. **82**, 5209 (1999), arXiv:hep-ph/9902483.

[21] V. Ravindran, J. Smith, and W. Van Neerven, Nucl.Phys. **B634**, 247 (2002), arXiv:hep-ph/0201114.

[22] C. J. Glosser and C. R. Schmidt, JHEP **0212**, 016 (2002), arXiv:hep-ph/0209248.

[23] J. M. Campbell, R. K. Ellis, and G. Zanderighi, JHEP **0610**, 028 (2006), arXiv:hep-ph/0608194.

[24] J. M. Campbell, R. K. Ellis, and C. Williams, Phys.Rev. **D81**, 074023 (2010), arXiv:1001.4495.

[25] V. Del Duca, W. Kilgore, C. Oleari, C. Schmidt, and D. Zeppenfeld, Nucl.Phys. **B616**, 367 (2001), arXiv:hep-ph/0108030.

[26] R. V. Harlander, T. Neumann, K. J. Ozeren, and M. Wiesemann, (2012), arXiv:1206.0157.

[27] I. M. Shoemaker and L. Vecchi, (2011), arXiv:1112.5457.

[28] M. T. Frandsen, F. Kahlhoefer, A. Preston, S. Sarkar, and K. Schmidt-Hoberg, JHEP **1207**, 123 (2012), arXiv:1204.3839.

[29] E. W. Kolb and M. S. Turner, *The Early Universe* (Westview Press, Chicago, 1994).

[30] N. Jarosik *et al.*, Astrophys.J.Suppl. **192**, 14 (2011), arXiv:1001.4744.

[31] M. Beltran *et al.*, Phys.Rev. **D80**, 043509 (2009), arXiv:0808.3384.

[32] E. Aprile *et al.* (XENON100 Collaboration), (2012), arXiv:1207.5988.

[33] J. Angle *et al.* (XENON10 Collaboration), Phys.Rev.Lett. **107**, 051301 (2011), arXiv:1104.3088.

[34] Z. Ahmed *et al.* (CDMS-II Collaboration), Phys.Rev.Lett. **106**, 131302 (2011), arXiv:1011.2482.

[35] D. Akerib *et al.* (CDMS Collaboration), Phys.Rev. **D82**, 122004 (2010), arXiv:1010.4290.

[36] R. Bernabei *et al.* (DAMA Collaboration), Eur.Phys.J. **C67**, 39 (2010), arXiv:1002.1028.

[37] C. Aalseth *et al.*, Phys.Rev.Lett. **107**, 141301 (2011), arXiv:1106.0650.

[38] To obtain the CoGeNT best-fit region, we have subtracted surface events from the total event rate as discussed in [39].

[39] C. Kelso, D. Hooper, and M. R. Buckley, Phys.Rev. **D85**, 043515 (2012), arXiv:1110.5338.